บทความวิจัย

การจำแนกความแก่ของส้มโอโดยใช้การวิเคราะห์ลักษณะของผิวเปลือกแบบต้นทุนต่ำและอัลกอริทึมการเรียนรู้ของเครื่อง

เกษรินทร์ ชาวเกวียน*
สาขาวิชาครุศาสตร์อุตสาหกรรม คณะวิทยาศาสตร์และเทคโนโลยี มหาวิทยาลัยราชภัฏนครปฐม
เอกนรา จันดา
คณะวิทยาศาสตร์และเทคโนโลยี มหาวิทยาลัยราชภัฏนครปฐม

* ผู้นิพนธ์ประสานงาน โทรศัพท์ 0 3410 9300 อีเมล: ketsarin@webmail.npru.ac.th DOI: 10.14416/j.kmutnb.2026.06.005
รับเมื่อ 25 พฤศจิกายน 2568 แก้ไขเมื่อ 7 กุมภาพันธ์ 2569 ตอบรับเมื่อ 12 มีนาคม 2569 เผยแพร่ออนไลน์ 15 มิถุนายน 2569

บทคัดย่อ

การขาดเครื่องมือที่มีความแม่นยำในการประเมินความแก่ก่อนการเก็บเกี่ยวถือเป็นปัญหาที่สำคัญสำหรับส้มโอ เนื่องจากส้มโอเป็นผลไม้ประเภทที่ไม่สามารถบ่มสุกได้ ซึ่งการพัฒนาคุณภาพภายในจะยุติทันทีเมื่อเก็บเกี่ยว ทำให้ความคลาดเคลื่อนในการตัดสินใจนำไปสู่ความสูญเสียทางเศรษฐกิจ งานวิจัยนี้นำเสนอกรอบแนวคิดแบบจำลองการเรียนรู้ของเครื่อง (Machine Learning) ที่มีต้นทุนต่ำสำหรับการจำแนกระดับความแก่ (ระยะเริ่มแก่และระยะแก่) ของส้มโอพันธุ์ขาวน้ำผึ้ง คณะผู้วิจัยได้รวบรวมชุดข้อมูลภาพทั้งหมด 1,008 ภาพ จากผลส้มโอ 70 ผล โดยถ่ายด้วยกล้องราสเบอร์รี่ ไพ (Raspberry Pi) ที่การเก็บเกี่ยว 2 ช่วง คือ 180 และ 210 วัน หลังติดผลเพื่อวิเคราะห์ความสัมพันธ์ระหว่างลักษณะภายนอกของผิวเปลือกและระดับความแก่ คณะผู้วิจัยได้วิเคราะห์คุณลักษณะด้านสีและพื้นผิวของเปลือกโดยใช้วิธีร่วมกับอัลกอริทึมซัพพอร์ตเวกเตอร์แมชชีน (SVM) ที่ใช้เคอร์เนลแบบฟังก์ชันฐานรัศมี (RBF) แบบจำลองที่พัฒนาขึ้นมีความแม่นยำในการจำแนกความแก่ภายใต้ชุดข้อมูลที่ไม่เคยเห็นอยู่ที่ร้อยละ 95.6 นอกจากนี้ผลการวิเคราะห์ความสามารถในการอธิบายผลลัพธ์ ยืนยันว่าการคัดแยกความแก่ของแบบจำลองสอดคล้องกับข้อมูลทางชีวภาพของส้มโอที่เกิดขึ้นจริง โดยระบุว่าความแปรปรวนขององค์ประกอบทางสี (ช่องสี b*) และลักษณะพื้นผิวละเอียด (LBP) เป็นตัวแปรที่สำคัญในการคัดแยกของแบบจำลอง งานวิจัยนี้แสดงให้เห็นว่าการวิเคราะห์คุณลักษณะของเปลือกด้วยเทคโนโลยีต้นทุนต่ำร่วมกับอัลกอริทึมการเรียนรู้ของเครื่องเป็นเครื่องมือที่มีความแม่นยำสูงสำหรับช่วยในการตัดสินใจเลือกช่วงเวลาเก็บเกี่ยวส้มโอที่เหมาะสม

คำสำคัญ: การคัดแยกความแก่ ส้มโอ การวิเคราะห์พื้นผิวภาพ แมชชีนเลิร์นนิง ระบบการมองเห็นต้นทุนต่ำ

การอ้างอิงบทความ: เกษรินทร์ ชาวเกวียน และ เอกนรา จันดา, "การจำแนกความแก่ของส้มโอโดยใช้การวิเคราะห์ลักษณะของผิวเปลือกแบบต้นทุนต่ำและอัลกอริทึมการเรียนรู้ของเครื่อง," *วารสารวิชาการพระจอมเกล้าพระนครเหนือ*, ปีที่ 36, ฉบับที่ 3, หน้า 1–15, ก.ค.–ก.ย. 2569, เลขที่บทความ 263-8231, doi: 10.14416/j.kmutnb.2026.06.005.

Research Article

Classification of Pomelo Maturity Using Low-Cost Peel Feature Analysis and Machine Learning Algorithms

Ketsarin Chawgien*
Industrial Education Program, Faculty of Science and Technology, Nakhon Pathom Rajabhat University, Nakhon Pathom, Thailand
Eknara Junda
Faculty of Science and Technology, Nakhon Pathom Rajabhat University, Nakhon Pathom, Thailand

* Corresponding Author, Tel. 0 3410 9300, E-mail: ketsarin@webmail.npru.ac.th DOI: 10.14416/j.kmutnb.2026.06.005
Received 25 November 2025; Revised 7 February 2026; Accepted 12 March 2026; Published online: 15 June 2026

Abstract

The lack of accurate pre-harvest maturity assessment tools is a critical challenge for pomelo production. Since pomelo is a non-climacteric fruit, its internal quality becomes fixed immediately upon harvest. Consequently, inaccuracies in harvest timing decisions directly result in economic losses. This study presents a cost-effective machine learning framework for maturity classification (early-mature vs. mature) of Khao Nampueng pomelos. A balanced dataset of 1,008 images from 70 pomelos was obtained using a Raspberry Pi camera at two critical times: 180 and 210 Days After Fruit Set (DAFS). To capture the non-linear relationships between peel appearance and maturity, color and texture features were analyzed using the Permutation Feature Importance method integrated with a Support Vector Machine (SVM) utilizing a Radial Basis Function (RBF) kernel. The proposed method yielded an optimized subset of biologically relevant features. The SVM-RBF model trained on this subset achieved robust classification performance, with a test accuracy of 95.6%. Interpretability analyses confirmed that the model's decision boundary aligned with physiological and biological changes, identifying variation in the chromatic component (b* channel) and micro-texture (LBP) as the most significant predictors. This study demonstrates that cost-effective peel feature analysis driven by machine learning algorithms provides a high-precision tool for optimizing pomelo harvest timing.

Keywords: Maturity Classification, *Citrus Maxima*, Image Texture Analysis, Machine Learning, Low-cost Vision System

Please cite this article as: K. Chawgien and E. Junda, "Classification of pomelo maturity using low-cost peel feature analysis and machine learning algorithms," *The Journal of KMUTNB*, vol. 36, no. 3, pp. 1–15, Jul.–Sep. 2026 (in Thai), Art. no. 263-8231, doi: 10.14416/j.kmutnb.2026.06.005.

1. Introduction

Pomelo, known as *Citrus maxima*, is a fruit product that has gained significant economic importance for Southeast Asian countries [1]. For example, Thai exports of pomelos are estimated to be over 25,000 tons in 2023 [2]. In particular, the Khao Nampueng variety is highly sought after due to its distinctive taste profile.

The non-climacteric physiology of pomelos is the primary factor limiting their commercial success. This is because the fruit's internal quality and sugar content cannot be improved after harvest. Consequently, premature harvesting results in a loss of quality, while harvesting at the optimal point ensures economic value. This requires dependable technology that can be used in the field to assess pomelo's maturity before harvesting efficiently [3]. The agricultural industry has increasingly applied modern technologies, such as precision agriculture and smart farming, to enhance crop management. For pomelos, these advances aim to replace conventional harvesting criteria, which are subjective and depend on visual evaluations of size, color, and oil glands, with objective judgments [4]–[6]. Today, Non-destructive Detection Technologies (NDT) combined with Artificial Intelligence (AI) are key to this transition, as they provide accurate, rapid, and consistent quality assessment [5], [7].

VIS/NIR spectroscopy is one of the most effective NDTs for predicting internal flavor attributes and acidity with high accuracy [8], [9]. Advanced approaches, such as X-ray imaging, show robust estimation of internal volume and flesh content, despite the high costs of hardware and operation, which limit field application. Artificial intelligence, particularly supervised Machine Learning (ML), has enhanced the quality assessment by identifying complex and non-linear patterns in the data without programming [5], [10]. Recent studies have integrated ML with image processing for pomelo quality assessment and orchard management. Sarakum and Sukpancharoen [2] developed a non-destructive framework for the classification of Khao Tang Kwa pomelos based on acoustic signal analysis and image features. Their study quantified oil gland density and peel thickness and used ensemble learning models to predict the internal quality. In the domain of field automation, Guan *et al.* [6] introduced Pomelo-Net, a predictive model based on an improved DeepLabV3+ architecture. Results showed that their method successfully addressed the challenges of identifying key orchard elements. Moreover, in the broader landscape of agricultural computer vision, Deep Learning (DL) models, particularly Convolutional Neural Networks (CNNs), have been established for automated fruit grading and have been successfully applied to crops such as apples and citrus. However, CNNs function as Black Boxes, require large datasets, and lack interpretability.

Even though NDTs provide highly accurate assessments, they often rely on costly, sensitive sensors that require precise operational settings, making them impractical for local farmers or small businesses, particularly in developing countries [2], [11], where they still heavily use manual, objective inspection. These limitations underscore the need for robust, low-cost alternatives that minimize operator restrictions. Leveraging ML techniques with image processing offers a promising strategy

for precision harvesting [12]–[15]. This approach provides a fast, non-contact, and scalable method for estimating the maturity using only a fruit's external appearance. Research studies have shown that color-texture characteristics and machine learning models can provide accurate and consistent quality grading of fruits, with the model's practical generalization [12], [16]. For pomelos, due to their non-climacteric nature, the harvest decision separating early-mature from mature pomelos is critical. Establishing a practical tool for this task would help farmers and small businesses optimize harvest timing, thereby reducing their reliance on costly and complex instruments.

We propose an interpretable machine learning framework to address a key challenge in precisely classifying the maturity of Khao Nampueng pomelos. The model is specifically designed to distinguish between the critical early-mature and mature stages. Using a low-cost Raspberry Pi camera, which is ideal for scalable field deployment and agricultural automation, our system extracts and quantifies peel color and texture features. These features undergo a careful selection process using Permutation Importance. They are optimized using a Support Vector Machine (SVM) with a Radial Basis Function (RBF) kernel. The goal is to create a non-destructive and cost-effective tool that provides a foundational component for optimal pomelo harvest-timing decisions.

2. Materials and Methods

2.1 Image Preparation

A total of 70 pomelos (Khao Nampueng) were picked from a farm in Nakhon Chai Si District, Nakhon Pathom Province, Thailand. These samples were preliminarily sorted into two maturity classes based on when they were picked: 35 fruits at 180 Days After Fruit Set (DAFS), designated as Early Mature, and 35 fruits at 210 DAFS, defined as Mature. All samples were sent to the lab within 24 h of harvesting.

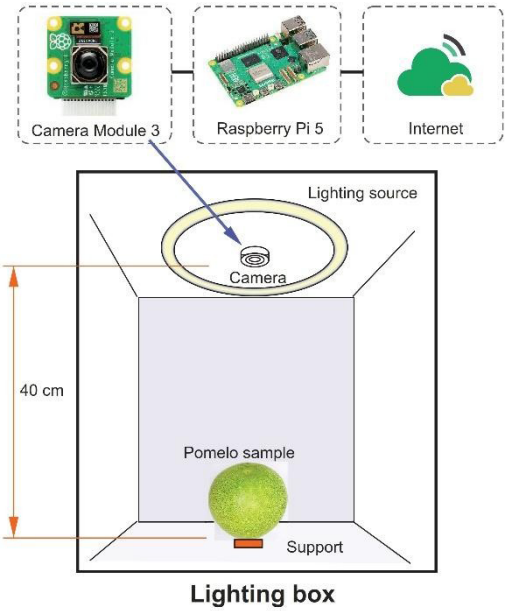

Figure 1 Schematic drawing of image setup.

Figure 1 shows the setup for the imaging accruing system. A lighting box (dimensions 50 × 50 × 45 cm) was used to control light intensity. We employed a circular LED ring light positioned around the camera lens. The light intensity was 750 ± 3 lux (measured at the lighting box floor). A matte white background was chosen to minimize specular reflections and maximize contrast. The camera (Raspberry Pi Module 3) was mounted directly above the sample platform at 40 cm. This Raspberry Pi camera was chosen because it is ideal for mobile robots or tight spaces, thanks to its compact size and lightweight design, making it

convenient for future automated detection systems. Moreover, its low cost is beneficial for scalable deployment or field applications where equipment might often be damaged.

For each sample, 18 images were taken. This was done by taking pictures from different angles around the sample, ensuring that the peel was fully shown. This included 8 images taken from the side, with the camera rotating 45 degrees between each one. The other images were taken at higher and lower angles, with each picture taken at 90-degree intervals. As a result of this process, a dataset of 1,008 high-resolution images was obtained (70 pomelo samples with 18 images each). This multi-view method provides a wide range of balanced data, ensuring general classification accuracy.

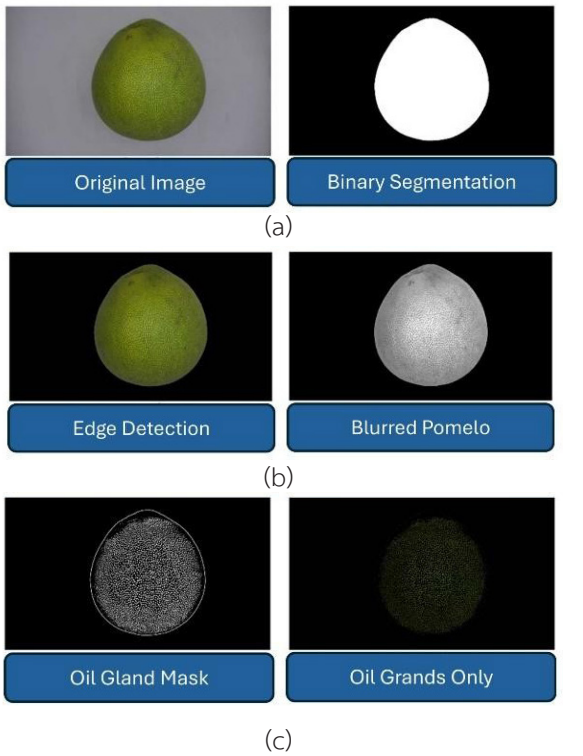

Figure 2 Pomelo's images analyzed using various processing techniques: (a) raw input and masked image, (b) edge detection operation and greyscale blurred image, and (c) image with oil glands detected.

2.2 Feature Extraction

The goal of feature extraction is to turn the raw pixel data from pomelo images into a set of numbers that can be used to build a classification model. We employed a multidomain approach to identify the fundamental chromatic, textural, and morphological features of pomelo peel associated with fruit maturity stage. Figure 2(a) illustrates the raw input image (Left) and the mask that separates the fruit from the background (Right). Figure 2(b), on the left, shows the result of applying an edge-detection operation, highlighting the fruit surface's boundaries and details. At the same time, a greyscale blurred version, prepared for texture detection, is presented on the right. Lastly, the oil glands detected are shown in Figure 2(c).

We used statistical data from the RGB and CIELAB color spaces to demonstrate how pomelo peel color evolves as it matures. The first and second statistical moments (Mean and Standard Deviation) of RGB features were calculated for each channel (R, G, and B) to explore the central tendency and variability of the color distribution across the peel surface. The means (R_{mean}, G_{mean}, B_{mean}) and standard deviations (R_{std}, G_{std}, B_{std}) can be calculated as Equations (1) and (2).

$$RGB_{mean} = \frac{1}{N}\sum_{i=1}^{N} p_i \quad ; RGB \{R,G,B\} \tag{1}$$

$$RGB_{std} = \sqrt{\frac{1}{N}\sum_{i=1}^{N}(p_i -)^2} \quad ; RGB \{R,G,B\} \tag{2}$$

where pi is the pixel value at location i and N is the total number of pixels in the peel region.

To reduce light variability and decrease the correlation among the RGB channels, pomelo images were converted to the CIELAB (L*a*b*) color space. By separating the achromatic lightness channel (L*) from the two chromaticity channels, a* (corresponding to the green-red axis) and b* (corresponding to the blue-yellow axis), it is easier to explore how the color of the peel changes with maturation, regardless of the light conditions [17]. Thus, we converted each RGB pomelo image to the L*a*b* color space, resulting in three component maps. After that, six statistical properties related to space were determined for each channel, including the mean (L*, a*, b*) and standard deviation (L*, a*, b*).

We also used statistics from local intensity gradients to obtain spatial information on the texture of pomelo peel, including the prominence and distribution of oil glands. This method measures the rate of change in pixel intensity across the surface of the fruit, related to edges (such as oil glands) and the texture's complexity. We used the Sobel operator to create a gradient magnitude map (G) from the horizontal (G_x) and vertical (G_y) gradients as expressed in Equation (3).

$$G = \sqrt{G_x^{\,2} + G_y^{\,2}} \tag{3}$$

The Gradient Mean ($Grad_{mean}$) and Standard Deviation ($Grad_{std}$) were then computed from this map using Equations (1) and (2).

Gray-Level Co-occurrence Matrix (GLCM) features were used to identify second-order spatial relationships among the pixel intensities of pomelo peel. We obtained the Haralick texture attributes Contrast, Homogeneity, Angular Second Moment, and Correlation. The characteristics were expected to relate to the distribution of oil glands or changes in texture as the fruit matures. We averaged the four GLCM characteristics over rotations of 0°, 45°, 90°, and 135° to represent our features. Each resulting GLCM, C, was normalized to create a probability matrix $P(i, j)$, where each element represents the joint probability of a specific co-occurrence, shown in Equation (4):

$$P(i,j) = \frac{C(i,j)}{\sum_i \sum_j C(i,j)} \tag{4}$$

Contrast (CON), Homogeneity (HOM), Angular Second Moment (ASM), and Correlation (COR) are defined as Equations (5)–(8), respectively:

$$CON = \sum_i \sum_j (i-j)^2 P(i,j) \tag{5}$$

$$HOM = \sum_i \sum_j \frac{P(i,j)}{1+(i-j)^2} \tag{6}$$

$$ASM = \sum_i \sum_j P(i,j)^2 \tag{7}$$

$$COR = \sum_i \sum_j \frac{(i-_i)(j-_i)P(i,j)}{_{i\,j}} \tag{8}$$

where μ_i, μ_j and σ_i, σ_j are the means and standard deviations of the row and column sums of $P(i, j)$, respectively.

Moreover, the micro-textural features of the pomelo peel, such as oil gland textures [18], were recorded using Local Binary Patterns (LBP). An LBP value map was generated using the decimal

representation of each pixel. This map was used to calculate two crucial features: the LBP Mean (LBP_{mean}) and the LBP Standard Deviation (LBP_{std}).

We have 20 features in total, covering all image-based descriptors. This composite set measures surface color, sharpness, and spatial-textural features for the model that sorts things by maturity. Here is a summary of the features.

Color features (12 total: R_{mean}, G_{mean}, B_{mean}, R_{std}, G_{std}, B_{std}, L^*_{mean}, a^*_{mean}, b^*_{mean}, L^*_{std}, a^*_{std}, b^*_{std})

Gradient features (2 total: $Grad_{mean}$, $Grad_{std}$)

GLCM features (4 total: CON, HOM, ASM, COR)

LBP features (2 total: LBP_{mean}, LBP_{std})

2.3 SVM-RBF classification framework

The first step in model development was preparing the data. Stratified sampling was used to randomly split the dataset into training and test sets. This strategy was used to maintain the same proportion of maturity classes in both the training and test sets [19]. The models were trained and tested on 80% of the database, while 20% was reserved for model validation. Z-score normalization sets the mean of the training dataset to 0 and its standard deviation to 1, enabling comparisons of features with different scales and units before training [20].

In this study, feature selection was performed to identify the subset of peel features that are most critical for distinguishing between early-mature and mature stages. We employed Permutation Feature Importance utilizing the SVM-RBF estimator. This wrapper-based method is preferred over simple filter-based techniques (e.g., ANOVA F-test) because pomelo biological growth such as oil gland micro-texture and color dispersion often involves complex, non-linear interactions that linear statistical metrics frequently fail to capture. The selection process began by training a baseline SVM-RBF model on the whole feature set, and the benchmark accuracy was recorded. Subsequently, the values of a single feature were randomly permuted across the validation samples. This permutation disturbed the link between that specific feature and the maturity labels, while keeping all other features constant. The model then re-evaluated the dataset, and the resulting decrease in classification accuracy informed the feature's predictive power. A significant drop implies that the feature is critical for defining the support vectors, whereas a negligible drop suggests the feature is redundant. This procedure reduces the feature space into the most efficient subset, reducing computational complexity while maintaining the separability between early-mature and mature classes.

To ensure the SVM-RBF model achieved maximum generalization performance, we tuned the two critical hyperparameters of the RBF kernel:

Regularization Parameter (C): This controls the trade-off between achieving a low training error and minimizing the norm of the weights. A properly tuned C prevents the model from overfitting outliers in the peel texture data.

Kernel Coefficient (γ): This defines the influence of a single training example. An optimized γ ensures the decision boundary captures the shape of the maturity data distribution.

We employed Grid Search with 5-fold cross-validation (GridSearchCV) on the training set to search for the hyperparameter space and identify

the optimal (C, γ) combination. The grid included a broad range of values.

$$C \notin \{0.1, 1, 10, 30, 100\}$$
$$\gamma \notin \{0.001, 0.01, 0.1, 1\}$$

Our final model was then retrained using these optimal parameters on the whole training set before being evaluated on the held-out test set. Their classification performance was examined, including precision, recall, accuracy, and F1 score (Equations (9)–(12)).

$$precision = \frac{TP}{TP + FP} \quad (9)$$

$$recall = \frac{TP}{TP + FN} \quad (10)$$

$$accuracy = \frac{TP + TN}{TP + FP + TN + FN} \quad (11)$$

$$F1 = \frac{2 \times precision \times recall}{precision + recall} \quad (12)$$

where TP is true positive, TN is true negative, FP is false positive, and FN is false negative.

3. Results and Discussion

3.1 Identification of Key Biological Features

The feature selection process using SVM-RBF with permutation importance successfully reduced the initial high-dimensional feature set to a subset of 15 key features. The reduction is expected in the application, which runs on low-cost embedded hardware (e.g., Raspberry Pi), thereby reducing memory usage and computation time for real-time, on-device inference without sacrificing accuracy. Figure 3 illustrates the improvement of the

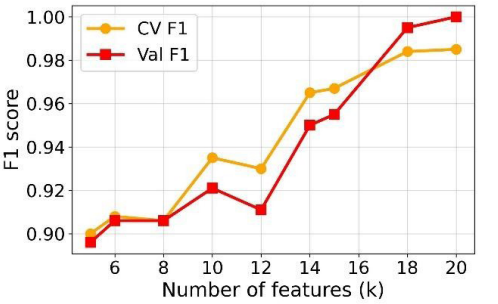

Figure 3 Score vs Number of features (k).

F1-score over different feature numbers. The plots show that the model performs well for k around 15, and that performance improves slightly when using nearly all features. While extending the feature set to include all available descriptors yields an approximately 1% gain in accuracy, it imposes a disproportionate computational burden due to its high computational intensity. Because feature extraction time is critical for resource-constrained edge devices like the Raspberry Pi, we determined that the selected 15-feature subset represents the optimal trade-off.

Permutation importance analysis was performed to quantify each feature's contribution to classification by the SVM–RBF model. Table 1 shows the metric indicating the mean decrease in classification performance when the feature values are permuted, averaged over 30 repetitions, with their standard deviations. Higher mean values indicate a greater impact on the performance.

The most essential features were the CIELAB blue–yellow component (b^*_{std}), followed by a^*_{std} B_{std} and LPB_{std} indicating that the variability of the blue–yellow (b*), red–green (a*), and Blue (B) channels, as well as Local Texture Variability (LBP) are the most influential predictors in the SVM–RBF

classifier. The features that had a moderate contribution to the model were ASM, $Grad_{mean}$, R_{mean}, b^*_{mean}, and CON, whereas global-intensity features such as Lmean and B_{mean} resulted in comparatively minor accuracy drops when permuted. These features reflected both the peel's surface texture and color transitions.

Table 1 Permutation importance

Features	Mean (%)	SD (%)
b^*_{std}	10.94	1.62
a^*_{std}	9.22	1.35
B_{std}	8.89	1.31
LBP_{std}	8.77	1.34
ASM	6.93	1.2
$Grad_{mean}$	6.26	1.17
R_{mean}	6.12	1.23
b^*_{mean}	6.12	1.63
CON	5.87	1.26
G_{std}	5.57	1.67
B_{mean}	5.25	1.1
HOM	4.33	0.97
L^*_{std}	4.31	1.48
R_{std}	3.94	1.29
L^*_{mean}	2.9	0.79

Finally, we identified a set of 15 features comprising color means regarding the yellowness axis (b*/B), color-channel variability (Standard deviation in R/G/B/L*/b*), texture metrics (HOM, COR, ASM), and edge structure (Gradient), as well as LBP capturing micro-texture. The combination suggests that the model is likely to be robust for model development. The list of features is ASM, G_{std}, $Grad_{mean}$, $Grad_{std}$, L^*_{std}, R_{std}, b^*_{mean}, B_{mean}, B_{std}, COR, HOM, b^*_{std}, CON, and LBP_{mean}.

3.2 Classification Performance

These 15 features mentioned above were used to develop the final SVM model with an RBF kernel. The hyperparameters used were C = 30 and γ = 0.1. The model was evaluated on an independent test set comprising 20% of the data. Note that this test set was never used during model training processes. Table 2 summarizes the key performance metrics on this test set.

Table 2 Performance of the SVM-RBF model

Performance	Data set	
	Training set	Test set
Precision CV	97.1%	95.7%
Recall CV	97.1%	95.6%
F1-score CV	97.1%	95.6%
Accuracy CV	97.1%	95.6%

This visual pattern is entirely consistent with the quantitative test-set metrics: a macro accuracy of approximately 95.6% and very similar macro precision, recall, and F1 scores. These values show that the model performs well and is balanced across both classes, rather than being biased toward a single maturity level.

The confusion matrix (Figure 4) for the hold-out test set provides further insight into the error distribution. Most of the samples are correctly classified, as reflected by the main diagonal of the matrix (true class = predicted class), indicating that the classifier well recognizes most fruits in both categories. A small proportion of samples appear in the off-diagonal cells, which represent misclassifications. These errors arose because the biological transition of fruits between maturity

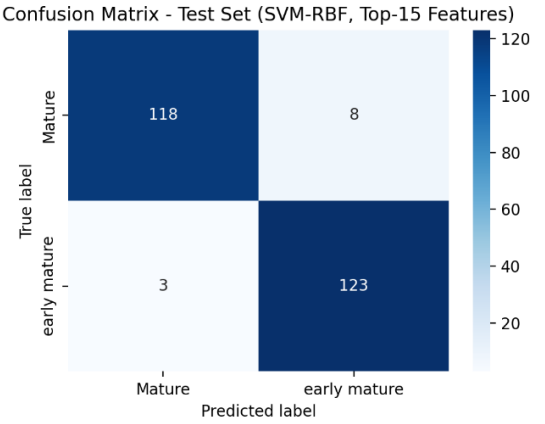

Figure 4 Confusion matrix.

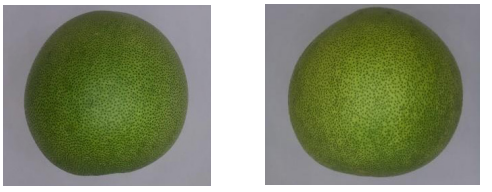

(a) (b)

Figure 5 Visual examples of classification performance: (a) Misclassification, and (b) Correct Classification.

stages is gradual rather than perfectly discrete. The peel's color, brightness, and texture are very close to the decision boundary, and slight variations can cause misclassification. Figure 5(a) shows that false negatives often involve mature fruits that retain high chlorophyll levels (low b* values) due to canopy shading or delayed yellowing, unlike the correctly classified sample (Figure 5(b)). In these cases, the strong chromatic signal overrides the micro-texture features (LBP), leading the SVM model to predict an early mature status.

From an application perspective, the confusion matrix indicates that the model is reliable enough to support automated grading or decision-support systems for pomelo maturity classification. Therefore, the confusion matrix suggests that the proposed SVM-RBF model with the selected peel features provides a robust tool for non-destructive assessment of pomelo maturity. It balances high overall accuracy with an error structure that is operationally acceptable for real-world grading scenarios.

3.3 Interpretation of the model using PDPs

The behavior of the SVM–RBF classification model was further examined using Partial Dependence Plots (PDPs) for the selected six key peel features: b^*_{std}, L^*_{std}, R_{std}, CON, $Grad_{mean}$, and LBP_{std}. PDPs visualize how the predicted probability of a given class changes as a single feature varies, while all other features are held at their observed values [21], [22]. In this study, the PDPs were computed with respect to the probability of the mature class. Hence, an increasing PDP curve indicates that larger values of a given feature push the model towards predicting the mature class. The PDPs (Figure 6) show that this model captures a coherent set of biological changes during maturation, including pigment dynamics, tissue structure, and surface micro-texture. In other words, the model classifies pomelos using the same cues that a trained human observes, but in a more quantitative way.

From a color perspective, the key features (b^*_{std}, L^*_{std}, R_{std}) can be understood in terms of pigment transformations in the peel. In the early mature stage, pomelo peel is still dominated by chlorophyll-rich green tissue, with carotenoids present but partly masked. As it matures, chlorophyll degrades, and carotenoids (yellow–orange pigments) become more visible, leading to a progressive

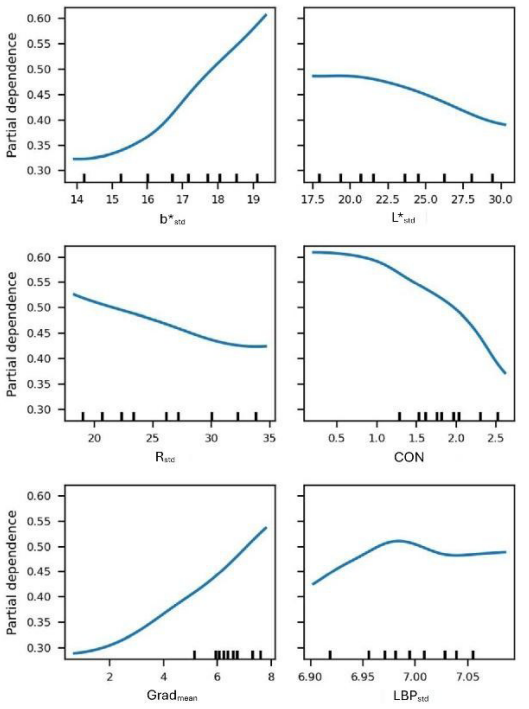

Figure 6 Partial dependence plots.

shift toward yellowish tones. The increases in the spatial variability of yellowish and moderate variation in reddish components (b^*_{std}, R_{std}) correspond to a higher probability of the mature class. Biologically, this suggests that during the transition phase, carotenoid expression is not uniform across the peel. Some regions lose chlorophyll and accumulate visible carotenoids earlier than others, creating a patchwork of slightly different yellow intensities. At the same time, the PDP for L^*_{std} indicates that mature fruits tend to have more uniform lightness than early mature ones. When the bright and dark patches disappear, the overall brightness across the surface becomes more even. That is, color itself becomes more complex in chromatic channels, but the underlying brightness distribution becomes smoother and less heterogeneous.

Texture-related features (CON, $Grad_{mean}$, LBP_{std}) reflect physical changes in the peel. Early in maturation, the peel surface typically shows more pronounced micro-relief: variations in oil gland prominence, small ridges, and local depressions, combined with uneven illumination and color distribution. These factors generate substantial regional differences in pixel intensity and texture. In the PDPs, higher CON values tend to decrease the probability of maturity. This is consistent with a surface that has sharp transitions (high gradients) along the edges of spots. As the fruit matures, the peel tends to become visually smoother. There is some evidence from citrus physiology that cuticle properties, water content, and turgor change during ripening, leading to flatter surface relief and a reduction of very sharp micro-edges. The waxy cuticle may redistribute or partially fill very fine irregularities, which the model recognizes as fruits mature. Moreover, the PDP for LBPstd shows that high micro-texture variability increases associated with maturation, whereas more homogeneous micro-texture is associated with the mature class. As the fruit approaches commercial maturity, the peel no longer exhibits as many abrupt micro-transitions, so the local patterns become statistically more similar across the surface, resulting in relatively stable LBPstd.

3.4 Comparison with Recent Pomelo Grading Methods

This section compares the classification accuracy of our proposed framework with that of a state-of-the-art approach by Sarakum and Sukpancharoen [2], which uses external peel

features as key features. Table 3 shows the key points of comparison. Sarakum and Sukpancharoen [2] achieved 93.9% accuracy in sweetness classification by combining acoustic resonance and morphological imaging. Their approach employs a complex mechanical setup to generate and record tapping sounds. In contrast, our results demonstrate that using only vision-based features achieves 95.6% accuracy. Furthermore, the model's accuracy is not the only advantage; the proposed system also offers operational scalability and simpler hardware.

Moreover, from an economic perspective, our proposed system provides significant benefits in scalability and accessibility. The estimated hardware cost for the developed acquisition setup is less than $500 USD. This contrasts with non-destructive VIS/NIR spectrometers or hyperspectral imaging systems, which generally cost exceeding $5,000 USD [4], [8]. By achieving high classification accuracy at low cost, this framework provides a practical solution for small-scale farmers and cooperatives.

Table 3 Comparative analysis with the recent state-of-the-art pomelo grading framework

Comparison Dimension	Proposed Method	Sarakum and Sukpancharoen [2]
Target Variable	Maturity (Binary: Early-Mature vs. Mature)	Sweetness (Binary: Sweet vs Unsweet)
Sensing Modality	Single-Source Image	Fusion (Acoustic Tapping + Image)
Algorithm	SVM-RBF	LightGBM
Dataset	1,008 Images	114 Images
Accuracy	95.6%	93.9%

4. Conclusion

This study proposes an image-based framework for pomelo maturity classification that relies primarily on peel information. The images are captured under controlled conditions using a Raspberry Pi, and their color and texture features are extracted using multiple image processing techniques to characterize peel appearance. A subset of informative peel features is then selected and used to represent key predictors associated with fruit maturation, and a Support Vector Machine with an RBF kernel (SVM-RBF) is trained to discriminate between early-mature and mature fruits. Finally, Partial Dependence Plots (PDPs) are used to visualize how each feature influences the predicted probability. In combination, this framework serves both as a non-destructive, automatable classification system and as an interpretable tool that quantitatively links peel features to biological changes in pomelo maturity.

The results demonstrated that peel-based color and texture features can effectively discriminate between Early-mature and Mature pomelos using a Support Vector Machine with an RBF kernel. By integrating a carefully designed image-processing pipeline with a non-linear classifier, the proposed method achieved high classification accuracy (95.6%) on an independent test set, indicating robustness and suitability for practical application in maturity assessment.

The analysis of Partial Dependence Plots provided significant insight into how the model's decision was linked with the biological transition of pomelos. Variation in chromatic components (b^*_{std} and R_{std}) and the uniformity of lightness (L^*_{std})

captured the progression from chlorophyll-dominated green peel to carotenoid-dominated yellow peel. Texture descriptors (CON, $Gradient_{mean}$, and LBP_{std}) reflected differences in irregular contrast and heterogeneous surfaces between early-mature and mature fruits. The consistency between these model-derived patterns and known physiological changes during pomelo maturation supports the biological plausibility of the classifier's decision rules.

From an application standpoint, the proposed method offers a non-destructive, automatable tool for grading pomelo maturity, potentially reducing reliance on manual inspection and improving consistency in harvesting. However, this study has some limitations. The model was developed under controlled imaging conditions and evaluated on a balanced dataset. Transitioning to field conditions requires considering lighting variability. While chromatic features dominate in controlled settings, we anticipate that texture-based predictors (LBP and GLCM) will be more robust against dynamic outdoor shadowing. Operational assessments confirm the feasibility of deploying this model on portable hardware, such as the Raspberry Pi 5. Empirical benchmarks demonstrate that the pipeline operates within real-time constraints, validating the system's potential for scalable, on-site application.

Furthermore, only external peel features were considered, while internal quality attributes such as total soluble solids and acidity were not directly modelled. Future research should focus on 1) testing and calibrating the model under real environments, and 2) integrating internal quality measurements.

5. Acknowledgement

This research was supported by Nakhon Pathom Rajabhat University under Grant DP66-11. The authors gratefully acknowledge this financial support.

References

[1] J. Yin, X. Hu, Y. Hou, S. Liu, S. Jia, C. Gan, Y. Ou, and X. Zhang, "Comparative analysis of chemical compositions and antioxidant activities of different pomelo varieties from China," *Food Chemistry Advances*, vol. 2, 2023, Art. no. 100180, doi: 10.1016/j.focha.2022.100180.

[2] T. Sarakum and S. Sukpancharoen, "Non-destructive sweetness classification of Khao Tang Kwa pomelos using machine learning with acoustic and image processing," *Journal of Food Composition and Analysis*, vol. 142, 2025, Art. no. 107385, doi: 10.1016/j.jfca.2025.107385.

[3] K. Chawgien and S. Kiattisin, "Machine learning techniques for classifying the sweetness of watermelon using acoustic signal and image processing," *Computers and Electronics in Agriculture*, vol. 181, 2021, Art. no. 105938, doi: 10.1016/j.compag.2020.105938.

[4] B. Lu, P. D. Dao, J. Liu, Y. He, and J. Shang, "Recent advances of hyperspectral imaging technology and applications in agriculture," *Remote Sensing*, vol. 12, no. 16, pp. 2659, 2020, doi: 10.3390/rs12162659.

[5] A. Koirala, K. B. Walsh, Z. Wang, and C. Mccarthy, "Deep learning – method overview and review of use for fruit detection and yield estimation," *Computers and Electronics in Agriculture*,

vol. 162, pp. 219–234, 2019, doi: 10.1016/j.compag.2019.04.017.

[6] X. Guan, H. Wan, Z. He, Z. Liu, R. Jiang, Y. Ou, Y. Chen, H. Gu, and Z. Zhou, "Pomelo-Net: A lightweight semantic segmentation model for key elements segmentation in honey pomelo orchard for automated navigation," *Computers and Electronics in Agriculture*, vol. 229, 2025, Art. no. 109760, doi: 10.1016/j.compag.2024.109760.

[7] D. Malowany and H. Guterman, "Biologically inspired visual system architecture for object recognition in autonomous systems," *Algorithms*, vol. 13, no. 7, pp. 167, 2020, doi: 10.3390/a13070167.

[8] H. Chen, H. Qiao, L. Xu, Q. Feng, and K. Cai, "A fuzzy optimization strategy for the implementation of RBF LSSVR model in Vis-NIR analysis of pomelo maturity," *IEEE Transactions on Industrial Informatics*, vol. 15, no. 11, pp. 5971–5979, 2019, doi: 10.1109/TII.2019.2933582.

[9] T. Jiang, J. Ding, Y. Du, S. Yuan, H. Yu, and W. Yao, "Deep learning-driven Vis/NIR spectroscopic devices for fruit quality assessment: A comprehensive review," *Trends in Food Science and Technology*, vol. 164, 2025, Art. no. 105262, doi: 10.1016/j.tifs.2025.105262.

[10] N. Upadhyay and A. Bhargava, "Artificial intelligence in agriculture : Applications, approaches , and adversities across pre-harvesting, harvesting, and post-harvesting phases," *Iran Journal of Computer Science*, vol. 8, no. 3, pp. 749–772, 2025, doi: 10.1007/s42044-025-00264-6.

[11] H. Wang, M. Mei, and J. Li, "Research progress on non-destructive detection of internal quality of fruits with large size and thick peel : A review," *Agriculture*, vol. 13, no. 9, pp. 1838, 2023, doi: 10.3390/agriculture13091838.

[12] S. S. Harakannanavar, J. M. Rudagi, V. I. Puranikmath, A. Siddiqua, and R. Pramodhini, "Plant leaf disease identification method using computer vision and machine learning algorithms," *International Conference on Integrated Intelligence and Communication Systems*, ICIICS 2023, vol. 3, pp. 305–310, 2023, doi: 10.1109/ICIICS59993.2023.10421345.

[13] G. Huang, Z. Xu, L. Liu, J. Chen, Z. He, and F. Liu, "Evaluating and deploying large vision-language models for fruit quality assessment in smart agriculture systems," *Computers and Electronics in Agriculture*, vol. 238, 2025, Art. no. 110806, doi: 10.1016/j.compag.2025.110806.

[14] E. Sheidaee and P. Bazyar, "Detection of white fig ripeness stages using deep learning models," *Iran Journal of Computer Science*, vol. 8, pp. 2935–2498, 2025, doi: 10.1007/s42044-025-00307-y.

[15] S. A. E. Kabel, W. El-shafai, F. E. A. El-samie, and B. Mohamed, "Enhanced plant identification and disease diagnosis through SqueezeNet and SVM for smart agriculture applications," *Iran Journal of Computer Science*, vol. 8, pp. 1353–1369, 2025, doi: 10.1007/s42044-025-00237-9.

[16] M. Soltani and F. Hamed, "Defect detection in fruit and vegetables by using machine vision systems and image processing," *Food Engineering Reviews*, vol. 14, no. 3, pp. 353–379, 2022, doi:10.1007/s12393-022-09307-1.

[17] A. K. Gupta, U. Pathak, T. Tongbram, M. Medhi, A. Terdwongworakul, L. S. Magwaza, A. Mditshwa, T. Chen, and P. Mishra, "Emerging approaches to determine maturity of citrus fruit," *Critical Reviews in Food Science and Nutrition*, vol. 62, no. 19, pp. 5245–5266, 2022, doi: 10.1080/10408398.2021.1883547.

[18] C. Wang, W. Suk, L. Xiangjun, Z. Daeun, and C. Hao, "Detection and counting of immature green citrus fruit based on the Local Binary Patterns (LBP) feature using illumination - normalized images," *Precision Agriculture*, vol. 19, no. 6, pp. 1062–1083, 2018, doi: 10.1007/s11119-018-9574-5.

[19] J. Neyman, "On the two different aspects of the representative method: The method of stratified sampling and the method of purposive selection," *Journal of the Royal Statistical Society*, vol. 97, no. 4, pp. 558–625, 1934, doi: 10.2307/2342192.

[20] E. Junda, C. Málaga-Chuquitaype, and K. Chawgien, "Interpretable machine learning models for the estimation of seismic drifts in CLT buildings," *Journal of Building Engineering*, vol. 70, 2023, Art. no. 106365, doi: 10.1016/j.jobe.2023.106365.

[21] E. Junda and C. Málaga-Chuquitaype, "Seismic acceleration demands in tall CLT buildings, predictive models and intensity measures," *Engineering Structures*, vol. 298, 2024, Art. no. 117024, doi: 10.1016/j.engstruct.2023.117024.

[22] S. Masís, Interpretable Machine Learning with Python. 2022, doi:10.1142/12774.